

- [19] H. Ago, K. Petritsch, M. S. P. Shaffer, A. H. Windle, R. H. Friend, *Adv. Mater.* **1999**, *11*, 1281.
- [20] H. Ago, M. S. P. Shaffer, D. S. Ginger, A. H. Windle, R. H. Friend, *Phys. Rev. B: Condens. Matter Mater. Phys.* **2000**, *61*, 2286.
- [21] K. Kim, S. H. Lee, W. Yi, J. Kim, J. W. Choi, Y. Park, J.-I. Jin, *Adv. Mater.* **2003**, *15*, 1618.
- [22] K. Kim, G. L. Zhong, J.-I. Jin, J. H. Park, S. H. Lee, D. W. Kim, Y. W. Park, W. K. Yi, in *Polymers for Microelectronics and Nanoelectronics*, ACS Symposium Series, Vol. 874 (Eds: Q. Lin, R. A. Pearson, J. C. Hedrick), ACS, Washington, DC **2004**, Ch. 2.
- [23] A. C. Ferrari, J. Robertson, *Phys. Rev. B: Condens. Matter Mater. Phys.* **2000**, *61*, 14095.
- [24] C. Yang, M. Wohlgenannt, Z. V. Vardeny, W. J. Blau, A. B. Dalton, R. Baughman, A. A. Zakhidov, *Phys. B (Amsterdam, Neth.)* **2003**, *338*, 366.
- [25] J. J. M. Halls, K. Pichler, R. H. Friend, S. C. Moratti, A. B. Holmes, *Appl. Phys. Lett.* **1996**, *68*, 3120.
- [26] S. M. Sze, in *Semiconductor Devices, Physics and Technology* (Ed: S. M. Sze), Wiley, New York **1985**, Ch. 9.
- [27] G. Yu, J. Gao, J. C. Hummelen, F. Wudl, A. J. Heeger, *Science* **1995**, *270*, 1789.
- [28] N. S. Sariciftci, D. Braun, C. Zhang, V. I. Srdanov, A. J. Heeger, G. Stucky, F. Wudl, *Appl. Phys. Lett.* **1993**, *62*, 585.
- [29] J. Y. Park, H. M. Le, G. T. Kim, H. Park, Y. W. Park, I. N. Kang, D. H. Hwang, H. K. Shim, *Synth. Met.* **1997**, *85*, 1239.
- [30] J. Y. Park, S. B. Lee, Y. S. Park, Y. W. Park, C. H. Lee, J. I. Lee, H. K. Shim, *Appl. Phys. Lett.* **1998**, *72*, 2871.
- [31] K. Kim, S. C. Jeoung, J. Lee, T. Hyeon, J.-I. Jin, *Macromol. Symp.* **2003**, *201*, 119.
- [32] T. Stubinger, W. Brutting, *J. Appl. Phys.* **2001**, *90*, 3632.

## Metallized Polyelectrolyte Microcapsules\*\*

By Dmitry G. Shchukin,\* Elena A. Ustinovich, Gleb B. Sukhorukov, Helmuth Möhwald, and Dmitry V. Sviridov

Nanostructured inorganic or hybrid organic/inorganic composites are important as they afford a direct connection between inorganic, organic, and biological materials. The ability to organize inorganic, organic, and biological components in a single composite material represents an interesting direction for developing multifunctional materials possessing a wide range of novel properties.<sup>[1]</sup> Among them, nanostructures with hollow interiors have been intensively studied for their appli-

cations as delivery and protection containers, fillers for bulk composite materials, and materials with unique optical or magnetic properties. Hollow nanostructures made of metals show surface-plasmonic properties (especially Au, Ag, and Cu) and catalytic activity superior to their solid analogs.<sup>[2]</sup> For instance, Halas and co-workers have demonstrated the tuning of the surface plasmon resonance band of a gold shell deposited onto a dielectric core (SiO<sub>2</sub>) from  $\lambda = 600\text{--}1200$  nm by changing the core diameter and thickness of the gold shell (for comparison, the surface plasmon resonance band of solid gold nanoparticles can be adjusted by about 50 nm at around  $\lambda = 520$  nm).<sup>[2b]</sup>

Hollow metal nanostructures are fabricated by coating the surface of a sacrificial template (e.g., Ag, SiO<sub>2</sub>, polymer latex).<sup>[3]</sup> However, the use of silica or polymer latexes as the template core results in the non-uniformity of the metal shell and makes the removal of the colloid templates without breaking the metal shell difficult. Hence, the portion of intact hollow metal structures is very low. Another more successful approach has been developed by Xia and co-workers.<sup>[4]</sup> This approach is based on the chemical substitution of silver atoms on the surface of a silver template particle by other, more electronegative metals (e.g., gold). As a result, the silver template reacts directly with a dissolved metal (gold) salt and is replaced by a hollow gold replica. Hollow gold nanostructures of different morphologies (spheres, triangular plates, cubes, rods, and wires) have been prepared by this metal-replacement procedure.<sup>[4]</sup> The drawback of this method, however, is the limited number of metals suitable for forming hollow replicas: only Au, Pt, and Pd nanostructures can be successfully synthesized, as other metals that are more electropositive than Ag (like Fe, Co, and Ni) cannot be reduced by elemental silver in a substitution reaction.

One of the recently developed protocols for inorganic synthesis is the preparation of inorganic nanomaterials inside spatially confined micrometer- or submicrometer-scale volumes of defined shape. An organized reaction microenvironment is employed to constrain and pattern inorganic precursors and to perform the synthesis of inorganic composites in a controllable and preselected way. A spatially confined microvolume allows one to carry out chemical syntheses under thermodynamic (energy) control, where the essential ingredients are present in the initial reaction mixture and the synthesis inside confined reactors is conducted in a parallel fashion; i.e., simultaneously in  $10^6\text{--}10^{10}$  compartments per milliliter.<sup>[5]</sup> Spatially confined micro- and submicroreactors avoid the influence of long-term kinetics, where the structure of the resulting nanomaterial would be governed by kinetic factors, thus causing inhomogeneities. Different types of microreactors (e.g., micelles,<sup>[6]</sup> liposomes,<sup>[7]</sup> microemulsions,<sup>[8]</sup> and gel microtemplates<sup>[9]</sup>) have been investigated and employed to synthesize composite inorganic nanoparticles.

Layer-by-layer-assembled polyelectrolyte capsules have been employed as excellent microreactors for carrying out the synthesis of magnetite, YF<sub>3</sub>, and hydroxyapatite exclusively in the inner volume.<sup>[10]</sup> It was found that the confined volume of

[\*] Dr. D. G. Shchukin, Dr. G. B. Sukhorukov, Prof. H. Möhwald  
Max Planck Institute of Colloids and Interfaces  
D-14424 Potsdam (Germany)  
E-mail: Dmitry.Shchukin@mpikg-golm.mpg.de  
E. A. Ustinovich, Prof. D. V. Sviridov  
Belarusian State University  
BY-220050 Minsk (Belarus)

[\*\*] This work was supported by the Sofja Kovalevskaja Program funded by the Alexander von Humboldt Foundation. D. S. acknowledges the Alexander von Humboldt Foundation for an individual research fellowship. The authors thank Dr. Jürgen Hartmann for EDX analysis.

the capsule microreactor affects the crystallinity, surface morphology, and particle size of the resulting substances. In addition, polyelectrolyte capsules composed of polyelectrolyte/inorganic shells have enhanced mechanical rigidity and maintain their bulky shape after drying whilst retaining the encapsulated compound inside.<sup>[11]</sup> Polyelectrolyte microcapsules were first reported in 1998.<sup>[12]</sup> They are fabricated by layer-by-layer adsorption of oppositely charged polyelectrolytes onto the surface of template microparticles.<sup>[13]</sup> Polyelectrolyte capsules are characterized by a high versatility of shell composition, facile fabrication, and control over capsule permeability. Depending on the size of the template particles, the capsule diameter can be varied from 50 nm to 20 μm or more. Besides polyelectrolytes, other materials (nanoparticles, biomaterials) could be constituents of the capsule shell, thereby providing additional functionalities (sensing, magnetism, fluorescence) and extending the applicability of the polyelectrolyte capsules.<sup>[14]</sup>

In the present communication, we investigate a new approach (the so-called “photocatalytic” approach) for the fabrication of both hollow and filled metal spheres that can be extended to other shapes and morphologies (rods, cubes, etc.). This approach is based on the spatially confined metallization of either the shell or the interior of polyelectrolyte capsules, which act as non-sacrificial template microreactors. Fabrication of nanostructured Ni spheres was taken as an example of the wider range of metals, as compared to the metal-replacement approach,<sup>[4]</sup> capable of being used to form hollow structured composites possessing interesting optical and magnetic properties.

The loading of polyelectrolyte capsules with metal nanoparticles could be carried out either by electrostatic adsorption during capsule assembly (employing the nanoparticles as one of the charged monolayers) or by direct synthesis in the microcapsules from the corresponding salts. The use of pre-formed inorganic nanoparticles (oxides, gold) as adsorbed shell monolayers has been demonstrated previously.<sup>[3b–3d]</sup> However, pre-formed nanoparticles aggregate inside the shell, and the mechanical properties of the capsule/pre-formed composites are similar to the properties of the individual components. In comparison, during the in-situ synthesis of nanosized

metals, a different morphology of the metal and synergetic effects of the confined microvolume are expected.

The metallization of polyelectrolyte capsules was performed in two stages to achieve homogeneous formation of Ni nanoparticles accelerated by the presence of the catalyst at the reaction site. In the first stage, a sublayer of heterogeneous TiO<sub>2</sub>/Pd catalytic centers was synthesized at the desired parts of the polyelectrolyte [poly(allylamine)/poly(styrene sulfonate), PAH/PSS] capsule. TiO<sub>2</sub> nanoparticles (4 nm) were then incorporated into the polyelectrolyte capsules to trigger the subsequent photochemical formation of catalytically active 1–2 nm Pd clusters on the surface (Fig. 1; a→b and a→e). Depending on the pH of the surrounding solution, TiO<sub>2</sub> can be adsorbed into the PAH/PSS shell (pH 5; Fig. 1, a→b) or be captured in the capsule volume (pH 2.5; Fig. 1, a→e). Active Pd clusters were produced by photocatalytic deposition of palladium (under UV irradiation<sup>[15]</sup>) from a 10<sup>-3</sup> M PdCl<sub>2</sub> solution onto the incorporated TiO<sub>2</sub> nanoparticles for 2 min (Fig. 1, b→c and e→f). This TiO<sub>2</sub>/Pd catalytic sublayer is necessary for fabrication of a uniform nanoparticulate Ni layer in the following stage, which is the electroless nickel plating. Nickel deposition was carried out using a hypophosphite-based nickel plating bath<sup>[16]</sup> in order to obtain a fine-grained nickel deposit in a slightly acidic medium (pH ≈ 6) and with moderate heating of the solution (55 °C); the deposition time was 2 min (Fig. 1; c→d and f→g). As a result, Ni deposition occurred exclusively on the sites where the TiO<sub>2</sub>/Pd catalyst was present to form polyelectrolyte capsules made of a dense polyelectrolyte/nano-Ni shell. Note that the direct metallization (without photoinduced formation of the catalytic sublayer) of the polyelectrolyte capsules activated by adsorption of Pd<sup>2+</sup> ions in the shell, followed by their reduction by hypophosphite, leads to the formation of large nickel aggregates that are weakly bound to the surface of the capsule (results not shown).

Transmission electron microscopy (TEM) images of the ultramicrotomed composite polyelectrolyte/nano-Ni capsules are shown in Figure 2. Figure 2a shows capsules containing reduced Ni nanoparticles only in the shell and not in the inner

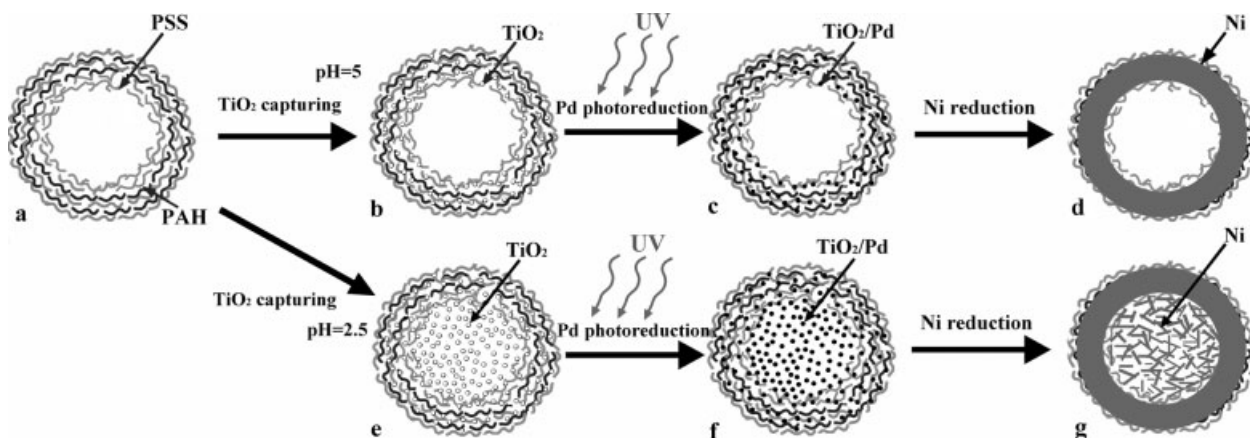
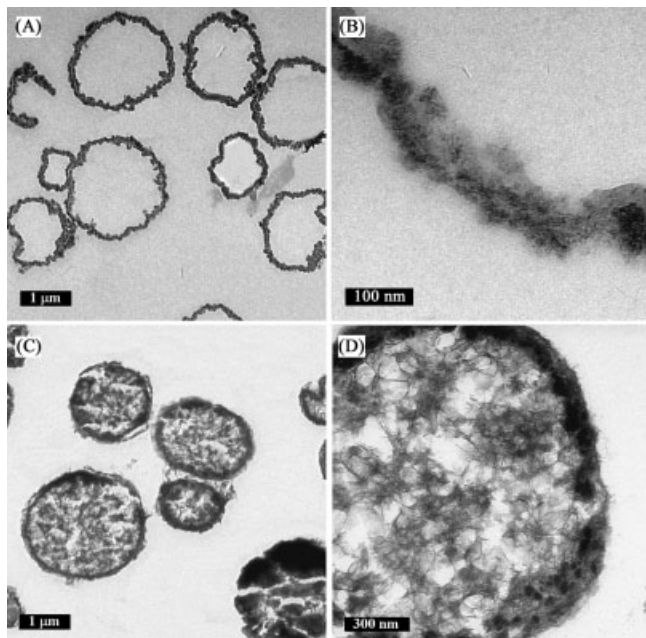


Figure 1. Schematic illustration of the synthesis of the composite polyelectrolyte/nano-Ni capsules at pH 5 and pH 2.5.



**Figure 2.** TEM image of the polyelectrolyte/nano-Ni capsules with Ni nanoparticles synthesized a,b) only in the shell and c,d) in both the shell and capsule microvolume. The samples were ultramicrotomed into ultra-thin sections (30–100 nm in thickness) using a Leica Ultracut UCT ultramicrotome.

volume. Here,  $\text{TiO}_2$  nanoparticles were adsorbed at pH 5, where they cannot penetrate the polyelectrolyte shell;<sup>[17]</sup> therefore, the Pd/ $\text{TiO}_2$  catalytic centers must be located only in the capsule shell. The shells of the thus-metallized capsules are dense and composed of closely packed 6–9 nm Ni particles.

Decreasing the pH of the colloidal solution during the  $\text{TiO}_2$  adsorption and Pd photodeposition step to 2.5 (Fig. 1; reaction sequence a→g) opens the polyelectrolyte shell so that  $\text{TiO}_2$  nanoparticles can be captured inside the capsule, where they do not aggregate or precipitate because of charge stabilization. This allows one to synthesize Ni nanoparticles not only in the capsule shell but also in the inner capsule volume. As shown in Figure 2c, the resulting polyelectrolyte/nano-Ni capsules are completely filled with Ni nanoparticles. There is a considerable difference in the shape and size between the nickel particles reduced in the shell and those in the interior volume of the capsule. Ni wires of about 10 nm in diameter and 100–200 nm long are formed in the capsule volume, whereas only small, spherical Ni nanoparticles about 7 nm in diameter are obtained in the capsule shell. A similar formation of Ni rods inside the confined microvolume of nanotubes has been reported by Bando et al.<sup>[18]</sup> This different particle morphology can be explained by the different conditions of crystallization in the capsule shell and inner volume, as shown previously for the synthesis of hydroxyapatite and magnetite inside polyelectrolyte capsules.<sup>[10,19]</sup> The small size and inner composition of the polyelectrolyte capsule affects the crystal structure and composition of the nanomaterial formed inside, which, as a consequence, can acquire specific properties that

differ from those of the corresponding nanomaterials prepared by conventional synthetic methods. The composite nature of the Ni-containing polyelectrolyte capsules was also confirmed by energy dispersive X-ray (EDX) analysis (Fig. 3). Reduced Ni nanoparticles, Ti from  $\text{TiO}_2$  nanoparticles, C, S, Na, and K from the PAH/PSS shell, and P from the hypophosphite derivative are observed in the EDX spectrum of the Ni capsules. The saturated magnetization of Ni nanoparticles entrapped inside the polyelectrolyte capsule is around  $35 \text{ A m}^2 \text{ kg}^{-1}$  at a magnetic field of 1 T. The coercivity value is 155 Oe ( $1 \text{ Oe} = 79.57 \text{ A m}^{-1}$ ).

The inorganic scaffold made of Ni nanoparticles in the capsule shell prevents capsule collapse after drying, producing stable, spherical metal capsules with morphologies and sizes reminiscent of those of the original polyelectrolyte capsules in solution (Fig. 4b), while polyelectrolyte capsules without the metal framework collapse to give flat, pan-like structures (Fig. 4a).

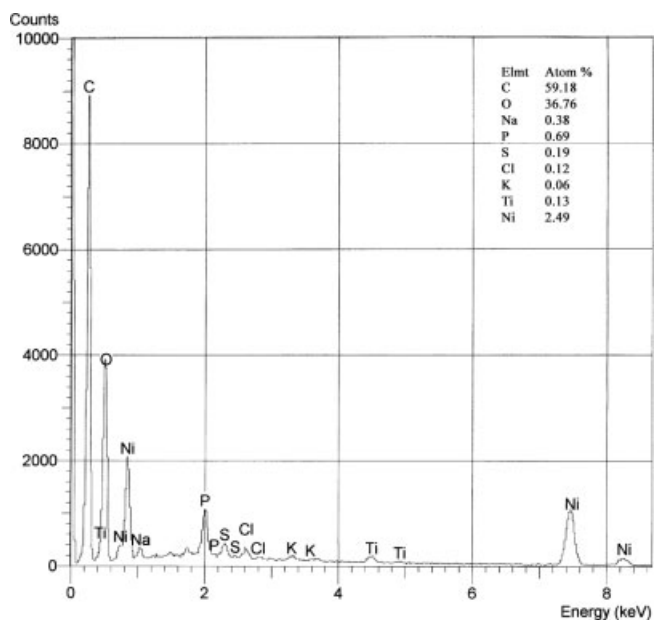


**Figure 3.** EDX analysis of polyelectrolyte/nano-Ni capsules. The EDX spectrum reveals nickel at 7.477 eV; Ni, Ti from  $\text{TiO}_2$ , C, S, Na, and K from the polymer shell, and P from the hypophosphite derivative are also observed.

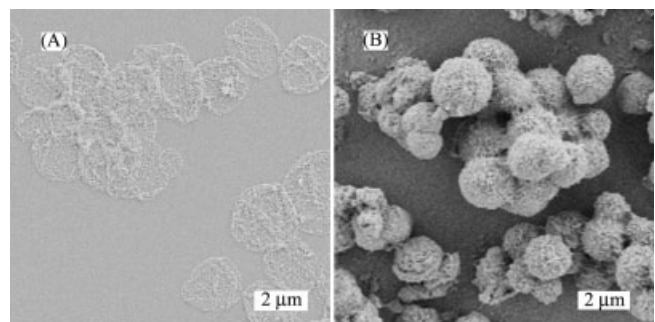


**Figure 4.** Scanning electron microscopy (SEM) images of a) the initial PAH/PSS capsules and b) polyelectrolyte/nano-Ni capsules with Ni nanoparticles in the shell.

Metal–polyelectrolyte capsules are capable of embedding different organic and bioorganic materials (drugs, polymers, enzymes, etc.) inside as they exhibit a synergistic superposition of the properties of the metal and polyelectrolyte phases. The permeability and release properties of the metallized capsules were investigated by employing fluorescein isothiocyanate (FITC)-labeled dextran (weight-average molecular weight  $M_w = 2000 \text{ kg mol}^{-1}$ ) as a probe. The open state for FITC-labeled dextran was observed at pH values below 3, whereas, at pH values above 4.5, dextran macromolecules cannot penetrate the capsule shell and remain entrapped (Fig. 5). As seen in Figure 5, the fluorescence signal has an even distribution throughout the whole capsule volume, which indicates the presence of freely floating FITC-labeled dextran inside the metallized capsules. Decreasing the pH to 2 leads to the release of the encapsulated dextran into the solution. The residual fluorescence observed from the capsule shell is due to the dextran molecules adsorbed on the shell, while all freely floating dextran was removed from the capsule volume. A similar permeability vs. pH dependence has been previously observed for PAH/PSS capsules.<sup>[17]</sup>

In conclusion, we have demonstrated that both hollow and filled Ni capsules can be synthesized by a “photocatalytic” approach with polyelectrolyte (PAH/PSS) capsules of  $2.2 \mu\text{m}$  diameter as template microreactors. This approach has several advantages over the other protocols employed to fabricate hollow metal micrometer- and submicrometer-sized objects (approx. 98 % yield, facile fabrication of template microreactors, and spatially resolved metal formation), and is widely applicable to the generation of particulate hollow metal structures involving different electropositive metals (Fe, Co, Zn, etc.). Depending on the synthetic route, the composite polyelectrolyte/nano-Ni capsules contain Ni nanoparticles either in the shell or in both the shell and the capsule interior volume. Because of the different crystallization conditions in the capsule shell and volume, Ni nanorods of about 10 nm in diameter with a length of 100–200 nm were formed inside the capsules, whereas only small spherical Ni nanoparticles of about 7 nm were obtained in the capsule shells. The metallized polyelectrolyte shell is pH sensitive and possesses pH-controlled permeability. The present metallized polyelectro-

lyte capsules could be used for galvanic deposition of metal–polymer composites, and are also of interest in optical and magnetic devices, as micrometer-sized catalysts containing nanostructured active materials, and as delivery microcontainers with shells sensitive to electromagnetic radiation. In the latter case, however, the toxicity of the metal nanoparticles should be considered. The magnetic and catalytic properties of the nano-Ni composite capsules, as well as the crystallization conditions inside the polyelectrolyte capsules, are currently under investigation.

## Experimental

**Materials:** Sodium poly(styrene sulfonate) (PSS, weight-average molecular weight  $M_w \approx 70\,000 \text{ g mol}^{-1}$ ), poly(allylamine hydrochloride) (PAH,  $M_w \approx 50\,000 \text{ g mol}^{-1}$ ),  $\text{PdCl}_2$ , nickel acetate, sodium acetate, fluorescein-isothiocyanate (FITC)-labeled dextran ( $M_w \approx 2\,000\,000 \text{ g mol}^{-1}$ ), HCl, and sodium hypophosphite were purchased from Aldrich. The synthetic protocol for fabrication of the  $2.2 \mu\text{m}$  monodisperse  $\text{MnCO}_3$  template particles was adapted from a previous synthesis [20], although it was carried out at higher temperature ( $70^\circ\text{C}$ ). All chemicals were used as received. The water was prepared in a three-stage Millipore Milli-Q Plus 185 purification system and had a resistivity higher than  $18 \text{ M}\Omega \text{ cm}^{-1}$ .

Hollow PAH/PSS capsules containing  $0.1 \text{ mol L}^{-1}$  of monomer units of PSS were prepared in two stages. In the first stage, a mixture of template  $\text{MnCO}_3$  particles and a  $0.01 \text{ M}$  solution of  $\text{Y}(\text{NO}_3)_3$  was made, and a  $5 \text{ mg mL}^{-1}$  PSS solution was added dropwise. The assembly of PAH/PSS multilayers on the top of the obtained  $\text{MnCO}_3/\text{PSS}$  particles was performed by the layer-by-layer technique from  $2 \text{ mg mL}^{-1}$  PAH and  $2 \text{ mg mL}^{-1}$  PSS solutions. After formation of the PAH/PSS shells, the  $\text{MnCO}_3$  core was dissolved in  $0.1 \text{ M HCl}$ . A more detailed description of the synthesis of PAH/PSS capsules can be found elsewhere [13].

The  $\text{TiO}_2$  nanoparticles were fabricated following a previously published procedure [21]. The inorganic precursor ( $\text{TiCl}_4$ ) was hydrolyzed by the addition of a 12.5 wt.-% aqueous ammonia solution with vigorous stirring of the solution at  $0^\circ\text{C}$ . The precipitate was centrifuged, washed with water, and, after adding nitric acid as a stabilizer, redispersed by sonication. The thus-prepared  $\text{TiO}_2$  colloid (concentration:  $7 \text{ g L}^{-1}$ ; average size of  $\text{TiO}_2$  particles:  $4 \text{ nm}$ ) did not exhibit any flocculation on standing for several months. Just before use, the acidity of the  $\text{TiO}_2$  colloid was decreased to pH 5.0 by dialysis. For impregnation with  $\text{TiO}_2$  particles, polyelectrolyte capsules were soaked in  $\text{TiO}_2$  colloid for three days at the corresponding pH and then washed thoroughly with water.

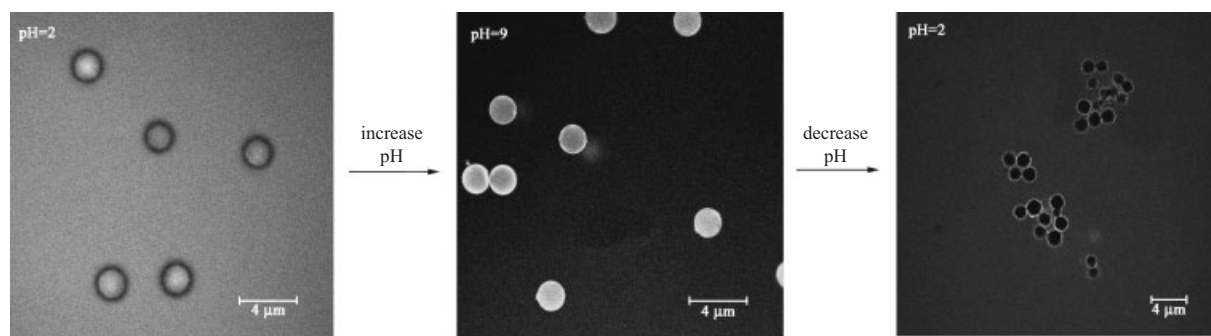


**Figure 5.** Confocal fluorescence microscopy images demonstrating the permeability of the polyelectrolyte/nano-Ni capsules towards FITC-labeled dextran ( $M_w = 2000 \text{ kg mol}^{-1}$ ). The figure confirms that pH-controlled permeability is preserved in the composite polyelectrolyte/nano-Ni capsules.

Electroless nickel deposition was performed at 55 °C from a plating solution containing nickel acetate (18 g L<sup>-1</sup>), sodium acetate (40 g L<sup>-1</sup>), and sodium hypophosphite (30 g L<sup>-1</sup>).

FITC-labeled dextran was incorporated into the capsule volume by varying the pH of the capsule suspension. Polyelectrolyte capsules were mixed with 0.2 mg mL<sup>-1</sup> FITC-labeled dextran solution at pH 2 (at this pH, the capsule shell is permeable to dextran macromolecules [17]). After 30 min of incubation, the pH was increased to 9 (at this pH, the capsule shell is in its "closed" state [17]) and the capsules were washed.

**Characterization:** For scanning electron microscopy (SEM) analysis, a drop of sample solution was applied to a glass wafer and dried at room temperature overnight. The material of the wafer did not influence on the morphology of the dried polyelectrolyte capsules. Then, the samples were sputtered with gold and measurements were conducted using a Gemini Leo 1550 instrument operating at an acceleration voltage of 3 keV. To view the nanoparticles composing the interior of the capsules, the samples were embedded in poly(methyl methacrylate) and ultrathin sections (30–100 nm in thickness) were obtained using a Leica Ultracut UCT ultramicrotome. Carbon-coated copper grids were used to support the thin sections, and a Zeiss EM 912 Omega transmission electron microscope (TEM) was employed for analysis. Confocal microscopy images of polyelectrolyte capsules in solution were obtained on a Leica TCS SP scanning system equipped with a 100× oil-immersion objective and operating in fluorescence mode. Energy dispersive X-ray (EDX) analysis was performed with a Zeiss DSM 940 scanning electron microscope.

Received: June 30, 2004

Final version: October 18, 2004

- [1] a) M.-J. Schwuger, K. Stickdorn, R. Schomaecker, *Chem. Rev.* **1995**, 95, 849. b) U. Schubert, N. Husing, A. Lorenz, *Chem. Mater.* **1995**, 7, 2010. c) P. Judeinstein, C. Sanchez, *J. Mater. Chem.* **1996**, 6, 511. d) D. S. Koktysh, X. Liang, B.-G. Yun, I. Pastoriza-Santos, R. L. Matts, M. Giersig, C. Serra-Rodríguez, L. M. Liz-Marzán, N. A. Kotov, *Adv. Funct. Mater.* **2002**, 12, 255. e) V. A. Sinani, D. S. Koktysh, B.-G. Yun, R. L. Matts, T. C. Pappas, M. Motamedi, S. N. Thomas, N. A. Kotov, *Nano Lett.* **2003**, 3, 1177. f) T. C. Wang, B. Chen, M. F. Rubner, R. E. Cohen, *Langmuir* **2001**, 17, 6610.
- [2] a) S.-W. Kim, M. Kim, W. Y. Lee, T. Hyeon, *J. Am. Chem. Soc.* **2002**, 124, 7642. b) J. B. Jackson, N. J. Halas, *J. Phys. Chem. B* **2001**, 105, 2473. c) S. J. Oldenburg, G. D. Hale, J. B. Jackson, N. J. Halas, *Appl. Phys. Lett.* **1999**, 75, 1063.
- [3] a) T. Ung, L. M. Liz-Marzán, P. Mulvaney, *Langmuir* **1998**, 14, 3740. b) F. Caruso, M. Spasova, V. Saigueirino-Maceira, L. M. Liz-Marzán, *Adv. Mater.* **2001**, 13, 1090. c) Z. J. Liang, A. Susha, F. Caruso, *Chem. Mater.* **2003**, 15, 3176. d) D. I. Gittins, A. S. Susha, B. Schoeler, F. Caruso, *Adv. Mater.* **2002**, 14, 508. e) Z. Zhong, Y. Yin, B. Gates, Y. Xia, *Adv. Mater.* **2000**, 12, 206.
- [4] a) Y. Sun, Y. Xia, *Science* **2002**, 298, 2176. b) Y. Sun, B. Mayers, Y. Xia, *Adv. Mater.* **2003**, 15, 641. c) R. Jin, Y. Cao, C. A. Mirkin, K. L. Kelly, G. C. Schalz, J. G. Zheng, *Science* **2001**, 294, 1901. d) P.-Y. Silvert, R. Herrera-Urbina, N. Duvauchelle, V. Vijayakrishnan, K. T. Elhsissen, *J. Mater. Chem.* **1996**, 6, 573.
- [5] a) M. P. Pileni, *Cryst. Res. Technol.* **1998**, 33, 1155. b) M. Antonietti, E. Wenz, L. Bronstein, M. Seregina, *Adv. Mater.* **1995**, 7, 1000. c) K. Landfester, *Adv. Mater.* **2001**, 13, 765.
- [6] a) M. C. McLeod, R. S. McHenry, E. J. Beckman, C. B. Roberts, *J. Phys. Chem. B* **2003**, 107, 2693. b) A. Martino, M. Stoker, J. S. Kawola, *Appl. Catal., A* **1997**, 161, 235. c) E. M. Egorova, A. A. Revina, *Colloid J.* **2002**, 64, 301. d) A. Martino, A. G. Sault, J. S. Kawola, M. Stoker, M. Hicks, C. H. Bartholomew, *Appl. Catal., A* **1997**, 161, 235. e) S. Klingelhofer, W. Heitz, M. Antonietti, *J. Am. Chem. Soc.* **1997**, 119, 10116.
- [7] A. Graff, M. Winterhalter, W. Meier, *Langmuir* **2001**, 17, 919.
- [8] a) T. Hirai, S. Hariguchi, R. J. Davey, *Langmuir* **1997**, 13, 6650. b) M. Li, S. Mann, *Adv. Funct. Mater.* **2002**, 12, 773. c) M. Willert, R. Rothe, K. Landfester, M. Antonietti, *Chem. Mater.* **2001**, 13, 4681.
- [9] a) J. H. Schattka, D. Shchukin, J. Jia, R. A. Caruso, M. Antonietti, *Chem. Mater.* **2002**, 14, 5103. b) R. A. Caruso, M. Giersig, F. Willig, M. Antonietti, *Langmuir* **1998**, 14, 6333. c) P. Korteso, M. Ahola, M. Kangas, M. Jokinen, T. Leino, L. Vuoriolehto, S. Laakso, J. Kiesvaara, A. Yli-Urpo, M. Marvola, *Biomaterials* **2002**, 23, 2795.
- [10] a) D. G. Shchukin, G. B. Sukhorukov, H. Möhwald, *Chem. Mater.* **2003**, 15, 3947. b) D. G. Shchukin, G. B. Sukhorukov, *Langmuir* **2003**, 19, 4427. c) D. Shchukin, I. Radchenko, G. Sukhorukov, *J. Phys. Chem.* **2003**, 107, 86.
- [11] a) D. G. Shchukin, G. B. Sukhorukov, *Adv. Mater.* **2004**, 16, 671. b) F. Dubreuil, D. G. Shchukin, G. B. Sukhorukov, A. Fery, *Macromol. Rapid Commun.* **2004**, 25, 1078.
- [12] E. Donath, G. B. Sukhorukov, F. Caruso, S. Davis, H. Möhwald, *Angew. Chem. Int. Ed.* **1998**, 37, 2202.
- [13] G. B. Sukhorukov, in *Novel Methods to Study Interfacial Layers*, (Eds: D. Möbius, R. Miller), Elsevier, Amsterdam, The Netherlands **2001**, p. 384.
- [14] A. Voigt, H. Lichtenfeld, G. B. Sukhorukov, H. Zastrow, E. Donath, H. Baumler, H. Möhwald, *Ind. Eng. Chem. Res.* **1999**, 38, 4037.
- [15] D. G. Shchukin, E. Ustinovich, D. V. Sviridov, Y. M. Lvov, G. B. Sukhorukov, *Photochem. Photobiol. Sci.* **2003**, 2, 975.
- [16] a) M. Tsuji, M. Hashimoto, T. Tsuji, *Chem. Lett.* **2002**, 12, 1232. b) F. Pearlstein, in *Modern Electroplating*, 3rd ed. (Ed: F. A. Lowenheim), Wiley, New York, **1974**, Ch. 31.
- [17] a) G. Ibarz, L. Dahne, E. Donath, H. Möhwald, *Adv. Mater.* **2001**, 13, 1324. b) A. A. Antipov, G. B. Sukhorukov, H. Möhwald, *Langmuir* **2003**, 19, 2444. c) G. B. Sukhorukov, A. A. Antipov, A. Voigt, E. Donath, H. Möhwald, *Macromol. Rapid Commun.* **2001**, 22, 44.
- [18] Y. Bando, K. Ogawa, D. Golberg, *Chem. Phys. Lett.* **2001**, 347, 349.
- [19] A. A. Antipov, D. G. Shchukin, Y. Fedutik, I. Zavaneskina, V. Klechkovskaya, G. B. Sukhorukov, H. Möhwald, *Macromol. Rapid Commun.* **2003**, 24, 274.
- [20] S. Hamada, Y. Kudo, J. Okada, H. Kano, *J. Colloid Interface Sci.* **1987**, 118, 356.
- [21] S. K. Poznyak, A. I. Kokorin, A. I. Kulak, *J. Electroanal. Chem.* **1998**, 442, 99.